PHYSICAL REVIEW B VOLUME 35, NUMBER 4 1 FEBRUARY 1987

Location of antimony in a halophosphate phosphor

K. C. Mishra, R. J. Patton, and E. A. Dale
GTE Electrical Products, Danvers, Massachusetts 01923

T. P. Das
Department of Physics, State University of New York at Albany, Albany, New York 12222
(Received 11 August 1986)

The location of antimony in halophosphate phosphors has been probed by use of ^{121}Sb Mössbauer spectroscopy. It has been shown that the observed Mössbauer parameters can be understood if the antimony is at the phosphorous site, its ligands being three of the oxygen atoms of the phosphate group and a fluorine ion. The problem of maintenance of the halophosphate phosphors in relation to loss of the fluorine ions and to the Sb^{5+} concentration associated with an impurity phase has also been studied.

I. INTRODUCTION

Antimony acts both as an activator and a sensitizer in the halophosphate phosphors used in fluorescent lamps.[1] In order to understand the activation and energy transfer processes[1] involving the antimony luminescent centers and the subsequent degradiation of the phosphor upon irradiation with ultraviolet photons, one needs the knowledge of the location of antimony in haloapatite and its interaction with the environment. However, structural information on the location of antimony in halophosphate phosphors is not currently available in the literature. In this paper, we report the results of our studies on the location of antimony in the fluorapatite crystal and some related systems based on theoretical analyses of the nuclear quadrupole coupling tensor and the isomer shift obtained from ^{121}Sb Mössbauer measurements.

The Mössbauer effect has often been used as a probe to obtain information on the electronic structure and local environment of impurities in solids.[2] The first attempt to utilize this technique for studying antimony impurities in halophosphate phosphor was made by Fraknoy-koros *et al.*[3] However, because the spectra were not resolved well enough to extract all of the Mössbauer parameters, their analyses were limited to the isomer shift only. Using the observed isomer shift for a variety of samples of commerical halophosphate phosphors, they were able to demonstrate the variations in relative abundance of Sb^{3+} to Sb^{5+} with respect to the quenching temperature, and also the existence of a second phase in the commerical phosphors. No attempt was made to use these experimental results to determine the location and electronic structure of antimony in halophosphate phosphors. In the present work we will present the results of our ^{121}Sb Mössbauer studies in a number of halophosphate phosphors. We have been able to obtain the nuclear quadrupole interaction parameters, i.e., e^2qQ and η, and isomer shift for the ^{121}Sb nucleus from the observed spectra. The experimental procedure and results will be discussed in detail in Sec. II.

The nuclear quadrupole interaction parameters[4] and the isomer shift[5] data carry the signature of the local electronic environment of the Mössbauer nucleus. In the past, theoretical interpretation of these data have provided valuable information regarding the electronic state and local environment of defects in solids.[2] In the present paper we shall describe our efforts to study the electronic structure associated with antimony using the cluster procedure. The electronic wave functions have been used to provide first-principles analyses of the nuclear quadrupole interaction data and isomer shifts. Details of the theoretical procedure used and the results of our analyses will be described in Secs. III and IV, respectively.

For our theoretical analyses, we have considered three different models describing the location of antimony in halophosphate phosphor.[6–8] These models ascribe antimony to different substitutional sites in apatite and have been proposed by various authors on the basis of stoichiometric and spectroscopic measurements. One of these models involves Sb^{3+} replacing Ca^{2+} at the Ca(II) site.[6] Such a substitution is accompanied by replacement of a neighboring F^- ion by one O^{2-} ion to maintain the charge neutrality. The second model involves a similar replacement at the Ca(I) site.[9] No model has been proposed describing the charge neutrality. The third model, originally proposed by Dale,[7] involves the substitution of a $(PO_4)^{3-}$ group by a $(SbO_3)^{3-}$ group. We have considered these three substitutional models in detail. As we shall discuss later, our results indicate strong support for the third model. We have considered explicitly the effect of lattice relaxation on the substitution of P^{5+} by the Sb^{3+} ion. On the basis of our analysis we have proposed that the Sb^{3+} ion is surrounded by three oxygen ions and one fluorine ion which are approximately 1.88 Å away from the antimony center. On the basis of this model, which we have utilized to interpret the Mössbauer data in the aged phosphors, a tentative explanation is proposed for degradation[1,10] of the halophosphate phosphors. In Sec. V, a brief summary of the results of our calculation will be presented.

II. EXPERIMENTAL PROCEDURE

A. Mössbauer parameters

The electric quadrupole interaction[4,5] results from the interaction between a nucleus of quadrupole moment Q

and an asymmetric electronic charge distribution described by the field gradient tensor q. In an arbitrary coordinate system the field gradient tensor is usually a nondiagonal symmetric real matrix. In the principal coordinate system, where the field gradient tensor is diagonal, the Hamiltonian representing this interaction is given by

$$H_Q=\frac{e^2qQ}{4I(2I-1)}\left[3I_z^2-I(I+1)+\frac{\eta}{2}(I_+^2+I_-^2)\right], \quad (1)$$

where I represents nuclear spin and

$$\begin{aligned} &I_\pm=I_x\pm I_y\ , \\ &q=q_{zz}\ , \\ &\eta=\frac{|q_{xx}|-|q_{yy}|}{|q_{zz}|}\ , \\ &|q_{yy}|\le|q_{xx}|\le|q_{zz}|\ . \end{aligned} \quad (2)$$

This interaction removes the nuclear spin degeneracy and leads to splitting of the Mössbauer spectrum. For the $I=7/2+$ to $5/2+$ transition for ^{121}Sb and a nonzero asymmetry parameter, the spectrum consists of 12 unresolved transitions. The transition frequencies and the amplitude of the various peaks as a function of e^2qQ and η are available in the literature.[11] A typical spectrum of Sb^{3+} in fluorapatite is shown in Fig. 1. The least-squares-fitting program, MROCOS (mathematical resolution of complex overlapping spectra) for resolving complex spectra to individual bands developed at Oak Ridge National Laboratory was modified to analyze the Mössbauer spectrum in order to obtain the hyperfine parameters. Each spectrum is fitted with 12 Lorentzians corresponding to the 12 peaks expected for a situation of nonzero asymmetry parameter. The relative separations and the heights of these peaks as a function of e^2qQ and η given by Shenoy and Dunlap[11] are used as constraints in the least-squares-fitting procedure. The hyperfine parameters and the widths of the Lorentzians are varied in order to obtain the best fitting of the theoretical curve to the observed spectrum.

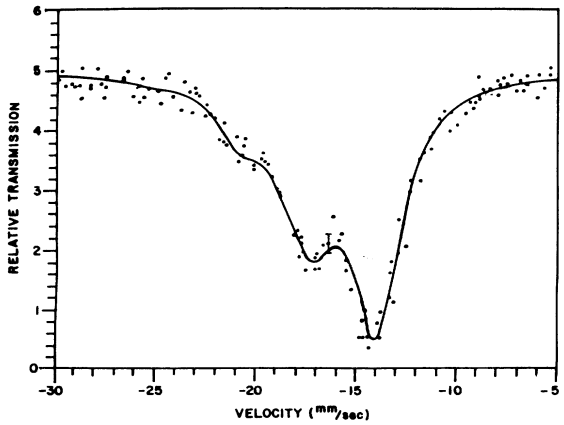

FIG. 1. The ^{121}Sb Mössbauer spectrum of fluorapatite. The error bars have been indicated on one of the data points in the figure.

The electronic isomer shift,[5] IS, results from the interaction of the electronic distribution with the charge distribution inside the nuclear volume. The shift in energy due to this interaction with respect to some specific compound used as the reference system is given by[12]

$$\Delta E_{IS}=\tfrac{2}{3}\pi ze^2(\Delta r^2)[\,|\Psi(0)|^2-|\Psi_r(0)|^2]\ , \quad (3)$$

where Δr^2 refers to the change in the radius of the nucleus undergoing the Mössbauer transition, z corresponds to nuclear charge, and $|\Psi|^2$ refers to the charge density at the nucleus. Since the isomer shift is usually expressed in mm/sec, one can rewrite Eq. (3) as

$$\Delta E_{IS}=\frac{2\pi C}{3E_\gamma}ze^2\Delta r^2[\,|\Psi(0)|^2-|\Psi_r(0)|^2]\ , \quad (4a)$$

$$\Delta E_{IS}=\alpha[\,|\Psi(0)|^2-|\Psi_r(0)|^2]\ , \quad (4b)$$

$$\alpha=\frac{2\pi C}{3E_\gamma}ze^2\Delta r^2\ . \quad (4c)$$

Obviously, α is a nuclear parameter and is a constant for a given nucleus. This is known in the literature as the isomer-shift calibration constant. The IS is a measure of the variation of the charge density at the nuclear site in different systems. The IS leads to a shift of the center of gravity of the Mössbauer spectrum which is relatively easier to measure than the quadrupole interaction parameters even when the spectrum is very complex.

B. Sample preparation

The experimental procedure of ^{121}Sb Mössbauer spectroscopy involving the 37.5-keV transition between $I=7/2+$ and $5/2+$ levels has been discussed elaborately in the literature.[13,14] Calcium stannate, $CaSnO_3$, obtained from New England Nuclear Corporation was used as the Mössbauer source. The phosphors studied using this technique were the following: fluorapatite (FAP): Sb, virgin fluor-chlorapatite (FClAP): Sb,Mn,Cd, which is commercially known as "cool white," and samples of "cool white" aged for 10^4 h. The Mössbauer measurements were also performed for Sb_2O_3 (orthorhombic) and antimony in the metallic form to test the accuracy of our measurements and reliability of the fitting routines. The values of e^2qQ, η, and IS obtained for these two systems were found to be in very good agreement with the values reported in the literature.[15] Measurements were also made on calcium antimonate, which is often found in halophosphate as an impurity phase,[16,17] and also on a number of samples of "cool white" having varying amounts of this phase. Our aim was to find from the Mössbauer spectrum any correlation between maintenance and amount of this second phase present in these samples. All of the phosphor samples used in our studies have been prepared at the GTE Phosphor Technology Laboratory. The measurements were performed at 50 K using fine particle size samples.

C. Experimental results

A typical Mössbauer spectrum for FAP is shown in Fig. 1. The spectrum is very well defined and characteris-

tic of the Sb^{3+} compounds. All the samples studied were analyzed for e^2qQ, and IS. The experimental values of these parameters along with the estimated error limits are presented in Table I. The quadrupole coupling constants showed only minor variations among the various halophosphates and were observed to be substantially larger than those that have been reported for the Sb^{3+} compounds with oxygen ligands. It can also be seen that the asymmetry parameters are in general nonzero for all the halophosphate phosphors, ruling out any substitutional site for antimony having threefold axial symmetry, such as the Ca(I) site.[18] There is also a slight increase in the value of e^2qQ as we go from FAP to FClAP and a decrease from the virgin to aged samples of "cool white." Further, the near equality of e^2qQ for the virgin and aged samples and the increase in η indicates that while the nature of electronic distribution surrounding antimony remains essentially unchanged, there may be some distortion in the lattice surrounding the impurity atom with the degradation of phosphor. Attempts will be made to understand this trend in order to determine the factors affecting the degradation of the phosphor.

Fraknoy-koros *et al.*[3] observed in their analyses peaks due to Sb^{5+} in FAP and FClAP, the relative concentration of which was noted to vary with the quenching temperature. From a comparison of the values of the IS corresponding to this center with that of calcium antimonate, $CaSb_2O_6$ they proposed that this compound forms a second phase in halophosphates. Similar propositions have also been made previously by other workers on the basis of x-ray and chemical studies.[16,17] However, in the commercial grade FAP and FClAP samples that we have studied no signals due to Sb^{5+} were observed. These materials are also known to have almost no second phase on the basis of chemical analysis.

The maintenance of a phosphor is defined as the ratio of the lumen output after time, t, to the initial lumen output.[1] It was considered worthwhile to investigate the effect of the second-phase compound on maintenance. Five different samples of "cool white" having varying amounts of the Sb^{5+} compounds were chosen for Mössbauer analysis. The maintenance characteristics of these samples were measured after 100 h of operation in a standard *F40/CW* fluorescent lamp. The ratio of the area of the peaks due to Sb^{5+} and Sb^{3+} centers is proportional to the ratio of Sb^{5+} to Sb^{3+} concentration.[3,5] Since the density of antimony atoms is equal to the sum of the densities for both the valence states, the ratio of the Sb^{5+} centers to Sb centers can be obtained from the ratio of the area of the peaks mentioned before. It was found that the phosphors having more Sb^{5+} centers degrade faster. An approximately linear relationship was noted between the ratio of Sb^{5+} to Sb concentration, C, and the logarithm of the maintenance, M, except for one point corresponding to a very high value of C (see Fig. 2).

On the basis of the linear variation of $\log_{10}M$ with respect to C, one can assume that there exists some kind of long-range interaction between these two different kinds of antimony centers which ultimately results in the degradation of phosphor. A possible mechanism for this interaction will be discussed in Sec. V. Before concluding this section, we would like to present an explanation of the observed linear relationship between C and $\log_{10}M$. We have examined two possible modes of degradation. They are (i) the change of the valence state of the antimony centers and (ii) structural changes in the environment of the Sb^{3+} sites rendering them inactive. We observed no signals for Sb^{5+} in aged "cooled white" samples after 10^4 h of operation. In view of this observation, it can be assumed that the process of degradation does not involve any change in the valence state of the activators. Near equality of the Mössbauer parameters observed for the aged and virgin "cool white" (Table I) appears to support the possibility that the process of degradation involves only structural changes leaving the valence state of the activator unaffected. Thus if N represents the density of the antimony centers, and m and n refer to those of the Sb^{5+} and Sb^{3+} centers,

$$N=m+n \ . \tag{5}$$

It is reasonable to assume that all the five samples have equal density of antimony atoms. Thus, N can be considered as a constant for all the samples. In view of the fact that some of the Sb^{3+} centers become passive in the course of the photodegradation, one can write

$$n=p(t)+q(t) \ , \tag{6}$$

where $p(t)$ and $q(t)$ refer to density of the active and passive centers at time t. The rate of change of active centers to passive centers will be proportional to m and $p(t)$. Thus,

$$\frac{dp}{dt}=-\alpha mp \ . \tag{7}$$

On solving Eq. (7) one can write

TABLE I. Summary of the experimental results obtained by ^{121}Sb Mössbauer spectroscopy.

Systems	ΔE_{IS} (mm/sec)	e^2qQ (mm/sec)	η
Fluorapatite (FAP)	-16.16 ± 0.11	23.00 ± 0.23	0.18 ± 0.03
"Cool white" (FClAP)	-16.20 ± 0.11	24.33 ± 0.23	0.18 ± 0.03
"Cool white" (aged 10000 h)	-16.08 ± 0.11	23.31 ± 0.23	0.22 ± 0.03
$CaSb_2O_6$	-0.69 ± 0.11	4.61 ± 0.23	0.60 ± 0.03[a]

[a]Calcium antimonate was studied at 4.5 K.

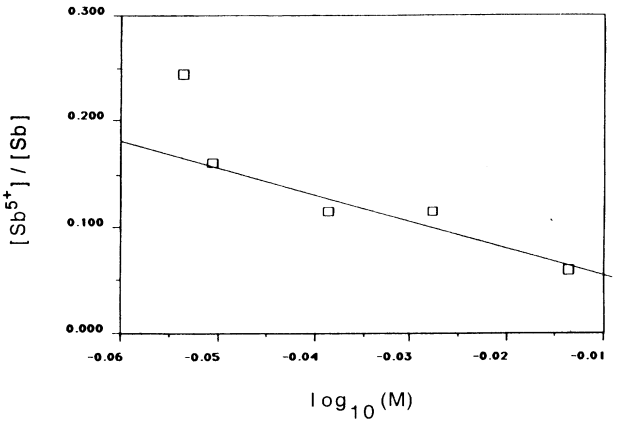

FIG. 2. The plot of logarithm of maintenance versus ratio of Sb^{5+} to Sb concentration.

$$\frac{p(t)}{p(0)}=\exp(-\alpha mt)=\exp(-\alpha' Ct)\ . \tag{8}$$

Maintenance being proportional to the quantity in the left-hand side of Eq. (8), the assumption of first order kinetics in Eq. (7) provides an explanation for the observed linear relationship between C and $\log_{10}M$ in Fig. 2.

It should be remarked that at this stage of our investigation it is not possible to confirm, on the basis of the Mössbauer data, the hypothesis that the Sb^{5+} centers correspond to the existence of calcium antimonate as an impurity phase.[3,16,17] Thus, the observed values of isomer shift for the Sb^{5+} centers in the "cool white" samples chosen were found to be very close to 0.0 mm/sec whereas for calcium antimonate it was measured to be approximately -0.69 mm/sec. Similar differences were observed by Fraknoy-koros *et al.*[3] in their analyses. In order to identify the chemical composition of the second phase without any ambiguity, more analyses are necessary.

III. THEORETICAL ANALYSIS

A. Description of clusters

The cluster procedure[2,19,20] has been used in the present calculations to interpret the Mössbauer parameters. The appropriateness of this approach for analyzing the local properties in solids such as the nuclear quadrupole interaction parameters[2] has been discussed in the literature. It is particularly suitable for studying the electronic properties associated with impurity atoms in ionic solids where the electrons are very localized. A cluster is like a giant molecule consisting of the impurity atom and atoms surrounding it with appropriate boundary conditions to simulate the effect of the rest of the crystal on the cluster. Thus one can treat the cluster by conventional molecular orbital procedures to calculate the electronic wave functions of the system.

In the present paper we have considered three possible models[6–9] describing the location of antimony in haloaphosphate phosphors. The geometry of the different clusters were chosen using the x-ray diffraction data[18] of halophosphates. We have used the same crystallographic notations in describing various sites in apatites throughout the paper.

The first cluster corresponds to the model involving the substitution of Ca^{2+} at the Ca(I) site by Sb^{3+} in halophosphate phosphors. The cluster consisted of one antimony atom, nine oxygen atoms, and three phosphorous atoms. The cluster has threefold symmetry characteristic[18] of the Ca(I) site. Any possibility of distortion of the lattice due to substitution of antimony has not been considered.

The second cluster consists of one antimony atom, ten oxygen atoms, and three phosphorous atoms. One of the oxygen atoms is at the fluorine site, necessary for charge compensation when Sb^{3+} is substituted for Ca^{2+} at the Ca(II) site.[6] This site was previously investigated using a similar procedure with clusters of comparable size in order to understand the emission and absorption spectra associated with the antimony centers in the haloapatites.[21]

The third cluster consisted of one antimony atom and three oxygen atoms. This cluster represents a model proposed by one of the authors[7] and assumes substitution of a PO_4^{3-} group by a SbO_3^{3-} group. In contrast to the other models, this picture suggests strong covalency in the bonding between antimony and oxygen atoms. In haloapatites, the phosphate group has three symmetry distinct oxygen atoms. Since for charge neutrality this model requires removal of one of the oxygen atoms, we considered all three of the possibilities. It is not possible at present to distinguish among the different oxygen atoms on the basis of quadrupole interaction data only. More theoretical and experimental efforts are necessary to identify the missing oxygen uniquely.

B. Theory of field gradient tensor

In order to understand the origin of the nuclear quadrupole coupling constant and the asymmetry parameter, one needs to calculate the field gradient tensor from the calculated electronic structure. In any arbitrary coordinate system, the components q_{ij} of the field gradient tensor are given by

$$q_{ij}=\sum_N \frac{\xi_N(3x_{iN}x_{jN}-r_N^2\delta_{ij})}{r_N^5}-\int\rho(r)\frac{3x_ix_j-r^2\delta_{ij}}{r^5}d\tau\ , \tag{9}$$

where i and j refer to x, y, and z coordinates, respectively. In Eq. (9), the first term represents contributions from the effective charges ξ_N at the nuclear sites. The quantities X_{iN} and y_{iN} refer, respectively, to ith and jth components of the radius vector joining the ^{121}Sb nucleus to another center being considered. The first term in Eq. (9) was multiplied by a factor of $1-\gamma_\infty$, where γ_∞ represents the Sternheimer antishielding factor[22] for antimony. In the present calculation, γ_∞ was chosen to be 14.00.[23] The second term represents the electronic contribution to the field gradient with $\rho(r)$ representing the electron density at r. In terms of the molecular orbital ψ_μ, $\rho(r)$ is given by

$$\rho(r)=\sum_\mu n_\mu\,|\,\psi_\mu\,|^2\ , \tag{10}$$

where n_μ denotes the population of the μth molecular or-

bital. The molecular orbitals ψ_μ are expressed as a linear combination of atomic orbitals, χ_i. Thus,

$$\psi_\mu = \sum_i C_{\mu i}\chi_i \ . \tag{11}$$

In evaluating the integral in Eq. (9) we kept only those terms which involved the atomic orbitals located at the antimony site. This gives the local contribution[24] of the electronic distributions to the field gradient tensor. The contributions arising from the nonlocal terms involving the atomic orbitals located at the other centers are usually very small and therefore have been neglected.

The molecular orbital coefficients in Eq. (11) have been calculated using the self-consistent charge extended Hückel (SCCEH) procedure.[25] This procedure has been described in the literature and will not be discussed here.

C. Theory of Isomer shift

In order to calculate the isomer shift, IS, one needs to calculate the charge density, $|\psi(0)|^2$, at the antimony site. We have used the self-consistent field multipole scattering (SCFMS) $X\alpha$ procedure[26,27] to obtain the charge density at the antimony sites. The contributions that arise due to the core and the valence electrons were calculated in a self-consistent manner. This method was preferred over the SCCEH procedure because the isomer shift involves a difference in charge densities between systems including the valence and core electrons. The core electron orbitals are frozen in the SCCEH procedure, which would preclude differences in core electron densities between different systems. Since the calibration constant[28] for antimony was not known precisely at the time of calculation, it was calculated using the IS data for two different simple systems. Using the calibration constant, α, thus calculated, the isomer shifts for ^{121}Sb in halophosphates were obtained and compared with experiment.

IV. RESULTS

A. Calculation of e^2qQ and η

As we mentioned before, our emphasis was on deriving structural information about the location of antimony in halophosphates through the interpretation of the nuclear quadrupole interaction parameters. When the quadrupole moment of the Mössbauer nucleus is precisely known, one can obtain the experimental value of the electric field gradient from e^2qQ. It is then possible to identify the location of the Mössbauer nucleus by comparing the observed field gradient tensor with those calculated from the electronic structure associated with the different models being considered.

However, the quadrupole moment of ^{121}Sb was not precisely known prior to our investigation. Several attempts have been made in the past to determine the quadrupole moment[14,29,20] Q of this nucleus from the experimental values of e^2qQ and estimated values of the field gradient at the antimony site. These attempts have led to a wide range of values (from -0.53 to 0.2 b) for the quadrupole moment of ^{121}Sb. These attempts involved quadrupole coupling constants obtained from techniques based on microwave spectroscopy,[29] atomic hyperfine structure measurements,[30] and nuclear quadrupole interaction studies using Mössbauer spectroscopy.[14]

In view of the large range of values of Q, we felt that it was important to determine Q from the electronic structures calculated by the SCCEH procedure taking advantages of the availability of the ^{121}Sb quadrupole coupling data for a number of simple molecular systems closely related to each other. For this purpose, the field gradient q was calculated at the antimony sites in SbH_3, SbF_3, $SbCl_3$, and $SbBr_3$ which were used to determine the quadrupole moment of the ^{121}Sb nucleus that best explains the quadrupole interaction data for these systems. The nuclear quadrupole interaction data for SbH_3 employed have been obtained by the molecular microwave technique[29] while for the other three systems e^2qQ were obtained from both the nuclear quadrupole resonance measurements and Mössbauer studies.[31]

On the basis of our analyses, the value of Q for ^{121}Sb was determined to be -0.29 b which provided the best agreement between theory and experiment for e^2qQ and η. The theoretical and experimental values of these parameters are presented in Table II for comparison. This value is identical with the one derived elsewhere from quadrupole interaction data in SbF_3 and Sb_2O_3 in the solid state from the Mössbauer studies combined with estimates of the field gradients in these systems.[14] It can be seen from Table II that the choice of $Q=-0.29$ b provides very good agreement between theory and experiment for all the systems except SbF_3. The experimental results for SbF_3 are also seen to differ substantially by the two different procedures. More experimental and theoretical efforts by first-principles procedures are needed to resolve these discrepancies. This value of Q was used in analyzing the quadrupole interaction data for halophosphates for which we have obtained the wave functions by the SCCEH procedure.

The field gradient tensors q_{ij} for the different models were calculated using Eq. (9). The field gradient tensors were then diagonalized to obtain q and η in the principal coordinate system following the conventions specified in Eq. (2). Summary of our results are presented in Table III. We will discuss our results in terms of the substitutional models that we have considered.

1. Ca(I) site

An examination of the energy levels and molecular orbitals corresponding to the cluster with antimony at the Ca(I) site indicates that the occupied energy levels with molecular orbitals having significant antimony character are rather delocalized and involve antimony $5s$ orbitals. The energy levels which involve molecular orbitals with antimony $5p$ character and which could have contributed significantly to the field gradient are unoccupied. It is therefore not at all surprising that this model leads to a very small value for e^2qQ (-2.01 mm/sec) for FAP compared to experiment. Furthermore, the sign of e^2qQ is opposite to the sign of the experimental value and η is 0.0 characteristic of the threefold symmetry of the Ca(I) site. In order to obtain a nonzero η one will have to distort the

TABLE II. Theoretical results for the ^{121}Sb quadrupole interaction parameters in SbH_3 and SbX_3 (X=F,Cl,Br) compared with experiment. The quantities inside the brackets refer to value of the quadrupole coupling constants measured in mm/sec expressed in the units of MHz.

System	Theoretical results e^2qQ	η	Experimental results e^2qQ	η
SbH_3	493.5 MHz	0.0	455.0 MHz	0.0
SbF_3	11.41 mm/sec	0.06	20.0 mm/sec	
			[587.0±28.0 MHz]	
			1073.0 MHz	0.03
$SbCl_3$	10.74 mm/sec	0.09	12.0 mm/sec	
			[365.0±51.0 MHz]	
			383.66 MHz	0.188
$SbBr_3$	8.93 mm/sec	0.116	9.0 mm/sec	
			[282.0±54.0 MHz]	
			343.95 MHz	0.1

lattice. However, it seems very unlikely that such distortions can lead to any significant improvement in e^2qQ to bring about good agreement with experiment which is an order of magnitude different.

2. *Ca(II) site*

The proposal suggesting the substitution of Ca^{2+} at the Ca(II) site by Sb^{3+} has been very popular. This model has been investigated using a 14-atom cluster. The nature of the molecular orbitals are found to be qualitatively similar to those obtained for the Ca(I) cluster. The quadrupole coupling constant (1.28 mm/sec) was found to be significantly smaller than the experimental value although the situation with the asymmetry parameter is better. Since η is a measure of the departure from the axial symmetry and there is evidence for this from the crystal structure data, the increase in η is not surprising. However, this model does not lead to an electronic distribution surrounding the Ca(II) site capable of producing the large field gradient at the antimony site. We also considered two extreme variations of this model before examining the phosphate model. One of the variations of the Ca(II) model refers to a situation in which antimony was considered to substitute Ca^{2+} and F^- ions as a Sb—O molecular fragment. In the other we considered a cluster con-

TABLE III. Summary of theoretical results for the quadrupole coupling interaction parameters.

Model	Cluster description	e^2qQ (mm/sec)	η
Ca(I) site	1Sb + 9O + 3P	−2.01	0.00
Ca(II) site	1Sb + 10O + 3P	1.28	0.48
	$(SbO_3)^{3-}$		
	d(Sb—O)=1.54 Å	19.47	0.03
PO_4 site	d(Sb—O)=2.10 Å	13.65	0.10
	d(Sb—O)=1.90 Å	17.39	0.75
	$(SbO_3)^{3-}F^-$		
	d(Sb—O)=1.90 Å	23.06	0.28
	d(Sb—F)=1.90 Å		
	d(Sb—O)=1.85 Å	23.66	0.04
	d(Sb—F)=1.85 Å		
	d(Sb—O)=1.88 Å	23.42	0.18
	d(Sb—F)=1.88 Å		
	$(SbO_3)^{3-}Cl^-$		
	d(Sb—O)=1.88 Å	28.20	0.03
	d(Sb—Cl)=2.34 Å		
	"Cool white"	24.38	0.15
	(0.8F + 0.2Cl)		
	$(SbO_3)^{3-}+e$	23.12	0.03
	Aged "cool white"[a]	23.32	0.12

[a]Quadrupole coupling constants for the aged sample were estimated as discussed in the text.

sisting of one unit of fluorapatite, $Ca_5F(PO_4)_3$ wherein Ca(II) was substituted by an antimony atom and the fluorine atom by one oxygen atom. In both the cases, e^2qQ was found to be comparable in magnitude to the values obtained by the original cluster and was an order of magnitude smaller from experiment. On the basis of these analyses we do not feel that this model describes the environment of antimony in apatite crystals.

3. PO_4 model

The nuclear quadrupole interaction parameters were obtained at the antimony site for the cluster representing the PO_4 model. The results presented in Table III correspond to the situation of the missing oxygen being an O(3). The removal of O(1) or O(2) changes the value of e^2qQ by less than 2%. Unlike the previous models, substantial $5p$ (antimony) character was observed among the occupied molecular orbitals. The calculated value of e^2qQ was found to be of comparable magnitude with experiment. This result is physically understandable because the absence of O(3) leads to strong departure from the tetrahedral symmetry for which the field gradient would have vanished. In fact, the relatively large size of the quadrupole coupling constant for ^{121}Sb can be understood in terms of the unbalanced p character in the direction of the missing Sb—O bond, which can produce a value of e^2qQ of approximately 16.80 mm/sec. The asymmetry parameter η was found to be very small compared to the experimental value. The small size of η is a result of near trigonal symmetry.

The PO_4 model thus provides a better explanation of the nuclear quadrupole coupling constant for ^{121}Sb than the other models, almost 85% of the observed value in FAP. We shall next discuss how one can derive some additional information about the nature of the environment of antimony in the PO_4 model from a consideration of the remaining 15% difference from the experiment.

In our investigations on the PO_4 model it was assumed that the Sb—O bond length was taken to be the same as the P-O distance observed by x-ray studies.[18] It is reasonable to expect that loss of an oxygen atom and substitution of a phosphorous atom by antimony which is a bigger atom will induce substantial lattice relaxation which would help to accommodate antimony in the apatite lattice. In view of this we considered the possibility of radial relaxation of Sb—O bond length, the results of which are included in Table III. It can be seen that the effect of relaxation is in general a reduction in the magnitude of e^2qQ moving theory away from experiment. However, it is very interesting to observe that the value of e^2qQ for the Sb-O distance of 1.90 Å is 17.30 mm/sec very close to 17.35 mm/sec observed for orthorhombic Sb_2O_3 system. This indicates (i) that the effect of relaxation is not an artifact of the calculation, (ii) that the SCCEH procedure is providing us with a reliable picture of the electronic distribution surrounding the antimony nucleus, and (iii) that the discrepancy between theory and experiment is real and suggests improvement over the model adopted.

It can be seen by examining the quadrupole coupling data for ^{121}Sb systems involving oxygen ligands only and with the antimony atom in trivalent state that e^2qQ varies between 17.0 and 19.0 mm/sec.[15] The calculated values of e^2qQ for FAP, including reasonable relaxations in the present model, lie within this range. On the other hand, in the case of SbF_3, e^2qQ is measured to be larger, namely 20.0 mm/sec. It is also seen from Table I that there is an increase in e^2qQ in going from FAP to FClAP. Both these facts suggest that the environment of antimony may include a halogen atom with which it has significant interaction. Since the apatite lattice contains fluorine and the fluorine ions are known to be rather mobile, we therefore examined the possibility of a fluorine ion being present in the vicinity of antimony, close enough to substantially affect the charge distribution of antimony. We considered two possibilities of lattice relaxation by choosing a SbO_3F^- cluster with oxygen and fluorine ions at identical distances, 1.85 and 1.95 Å from antimony. The fluorine atom was found to be in a charge state of -0.98, indicating an ionic interaction between the SbO_3 group and fluorine ion. The calculated values for e^2qQ and η for these two clusters are in excellent agreement with experiment. Using η to determine the Sb-O distance, best agreement between theory and experiment was obtained for a Sb-O distance of 1.88 Å, which agrees well with the observed antimony oxygen bond length in a number of inorganic antimony compounds.[32] It is interesting to note that similar kinds of relaxation have been observed in various systems, the atoms surrounding the impurity relaxing in such a manner that the distance between the impurity and the nearest-neighbor atoms corresponds to the situation of covalent bonding.[2] In view of the fact that the F^- ion is bonded ionically to antimony and not covalently, the increase in e^2qQ can be understood in terms of a repulsion of charge density between the two groups which results in a building up of charge density at the antimony site. If this explanation is right, we would also expect an enhancement in e^2qQ in the presence of a Cl^- ion because of the greater electronic repulsion arising from its larger size. This was indeed what we found from our calculations on the SbO_3Cl^- cluster (Table III). Since the halogen component of FClAP is composed of approximately 80 at.% F^- ion and 20 at.% Cl^- ion, one could estimate the value of e^2qQ for this system by combining the quadrupole coupling constants in similar ratio. This leads to a value of e^2qQ equal to 24.38 mm/sec which is very close to the experimental value (Table I).

Before terminating this subsection we would like to make some comments on the ^{121}Sb quadrupole interaction in degraded phosphors. The E(II) type[33] of color centers involving trapping of an electron at F^- vacancies have often been associated with the degradation of phosphor. We have considered the effect of formation of an E(II) center close to an antimony center on the quadrupole coupling constant. This leads to a value of e^2qQ of 23.42 mm/sec. We have used this value and the calculated values of e^2qQ for FAP and FClAP in Table III to make an estimate of the coupling constant for the degraded "cool white" assuming that 20% of the Sb^{3+} with FAP environment have become passive due to aging. For this purpose, one can consider 64% of nuclei as having FAP environment, 16% as being adjacent to the E(II) centers,

TABLE IV. Summary of charge density in a.u. and IS in mm/sec.

Systems	Charge density (a.u.)	ΔE_{IS} (Expt.) (mm/sec)	ΔE_{IS} (Theor.) (mm/sec)
SbF_3	93 287.646	−14.6	
Sb_2O_3	93 285.581	−11.32	
FAP (PO_4 model)	93 289.544	−16.16	−17.61

and 20% as being in an environment similar to ClAP. This leads to a value of 23.32 mm/sec in excellent agreement with experiment (Table I). In view of this agreement, we believe that there exists some correlation between loss of the fluorine ions and maintenance. This question should be pursued further with more experiments and theoretical efforts.

B. Isomer shift

We have carried out theoretical analyses to utilize the experimental data on isomer shift as a check on the model discussed in the preceding section for the location of antimony in FAP. Unfortunately, at the time of investigation the calibration constant for ^{121}Sb was not available. Therefore we calculated the latter using the isomer shift data for Sb_2O_3 and SbF_3 and the theoretical values of charge densities at the antimony site using the SCFMS$X\alpha$ procedure. The theoretical values for charge densities at the antimony site for Sb_2O_3, and FAP using the SbO_3F^- model are given in Table IV. The charge densities at the antimony site in Sb_2O_3 and SbF_3 were used to calculate the calibration constant for the ^{121}Sb nucleus. The calibration constant was found to be $1.59a_0^3$ sec/mm. Using Eq. (4b) the IS for FAP was found to be 17.61 mm/sec, in very good agreement with experiment. It is interesting to note that the IS for FAP was more than in Sb_2O_3 and SbF_3 which lends support to our finding that in FAP the environment of antimony involves more than three oxygen atoms only. The inclusion of the fluorine ion in the environment of antimony not only explains the experimental value of IS but also explains the trend as we go from Sb_2O_3 to SbF_3 to FAP.

V. CONCLUSION

The theoretical studies of the Mössbauer parameters for ^{121}Sb nucleus have led to a unique picture of the location and environment of antimony in halophosphate phosphor. The $(SbO_3)^{3-}F^-$ model which was found to provide a very consistent explanation of the observed Mössbauer parameters highlights two very interesting aspects of the antimony centers in the halophosphate phosphors. They are (i) the covalent nature of bonding between antimony and its oxygen neighbors and (ii) the importance of the halogen ligands. It is our conjecture on the basis of the Mössbauer data for the aged materials that the F^- ions are lost during the process of photodegradation. What exactly happens to the missing fluorine ions will be a very interesting problem to pursue experimentally. In view of the fact that the presence of a second phase accelerates the process of degradation, it is possible that the highly mobile fluorine ions migrate to the domains of the second phase which, being an impurity, is far from the stoichiometric composition and thus can be expected to have numerous vacancies. It will be interesting to analyze the composition of this phase chemically for virgin and aged samples of identical phosphors in order to find out if it provides a sink for the fluorine ions. The loss of the fluorine ions is not necessarily the only mechanism of degradation of the halophosphate phosphors. Many different mechanisms have ben proposed in the literature describing the process of deterioration of phospor in fluorescent lamps. One can indeed notice a significant departure from the linear relation proposed on the basis of Eq. (8) at the maintenance decreases (Fig. 2). However, the loss of fluorine ions is expected to be one of the dominant modes of photodegradation.

Our analyses thus have led to a new understanding of the halophosphate phosphors. It is very important that various electronic processes involving the antimony centers should be reinvestigated in view of this new model. For example, the mechanism of energy transfer from antimony to manganese centers, which otherwise would not fluoresce would be an interesting problem to be reexamined. It is hoped that such analyses will lead to better understanding of phosphors and also to the exploration of novel ways of manufacturing better phosphors.

[1]K. H. Butler, *Fluorescent Lamp Phosphors, Technology and Theory* (Pennsylvania State University Press, University Park, 1980).

[2]M. Van Rossum, I. Dezsi, K. C. Mishra, T. P. Das, and A. Coker, Phys. Rev. B **26**, 4442 (1982); M. Van Rossum, G. Langouche, K. C. Mishra, and T. P. Das, *ibid.* **28**, 6086 (1983).

[3]V. Fraknoy-koros, G. Gelencser, B. Levay, and A. Vertes, J. Lumin. **9**, 467 (1975).

[4]T. P. Das and E. L. Hahn, *Nuclear Quadrupole Resonance Spectroscopy* (Academic, New York, 1957), Suppl. 1.

[5]G. M. Bancroft, *Mössbauer Spectroscopy* (McGraw-Hill, London, 1973).

[6]J. L. Ouweltjes, Phillips Tech. Rev. **13**, 346 (1952); A. H.

Hoekstra, Ph.D. thesis, Technical University, Eindhoven, 1967; W. D. Partlow and J. Murphy, Bull. Am. Phys. Soc. **15**, 372 (1970); T. S. Davies, E. R. Kreidler, J. A. Parodi, and T. F. Soules, J. Lumin. **4**, 48 (1971).

[7]E. A. Dale (private communication).

[8]For a brief review of the various sites, see P. D. Johnson, in *Luminescence of Organic and Inorganic Materials,* edited by H. P. Kallmann and G. M. Spruch (Wiley-Interscience, New York, 1962).

[9]Reference to the Ca(I) site can be found in R. W. Warren, F. M. Ryan, R. H. Hopkins, and J. N. Broekhoven, J. Electrochem. Soc. **122**, 752 (1975).

[10]E. F. Lowry, Illum. Engineering **44**, 98 (1948).

[11]G. K. Shenoy and B. D. Dunlap, Nucl. Instrum. Methods. **71**, 285 (1969).

[12]B. D. Dunlap and G. M. Kalvius, in *Mössbauer Isomer Shifts,* edited by G. K. Shenoy and F. E. Wagner (North-Holland, New York, 1978).

[13]R. E. Snyder and G. B. Beard, Phys. Lett. **15**, 264 (1965).

[14]S. L. Ruby, G. M. Kalvius, G. B. Beard, and R. E. Snyder, Phys. Rev. **159**, 239 (1967).

[15]N. N. Greenwood and T. C. Gibb, in *Mössbauer Spectroscopy* (Chapman and Hall, London, 1971), p. 444.

[16]W. L. Wanmaker and M. L. Verheyke, Philips Res. Rep. **11**, 1 (1956).

[17]K. H. Butler, M. J. Bergin, and V. M. B. Hannaford, J. Electrochem. Soc. **97**, 117 (1950) and references therein.

[18]P. E. Mackie and R. A. Young, J. Appl. Crystallogr. **6**, 26 (1973).

[19]K. Herman and P. S. Bagus, Phys. Rev. B **20**, 1603 (1979) and references therein.

[20]N. Sahoo *et al.*, Phys. Rev. Lett. **50**, 913 (1983).

[21]T. F. Soules, T. S. Davis, and E. R. Kreider, J. Chem. Phys. **55**, 1056 (1971).

[22]See, for instance, R. M. Sternheimer, Phys. Rev. **130**, 1423 (1963); **132**, 1637 (1963); P. C. Schmidt, K. D. Sen, and T. P. Das, Phys. Rev. B **22**, 4167 (1980).

[23]E. H. Hygh and T. P. Das, Phys. Rev. **143**, 452 (1966).

[24]A. C. Beri, R. M. Sternheimer, T. Lee, and T. P. Das, Phys. Rev. B **28**, 2335 (1983).

[25]R. Hoffmann, J. Chem. Phys. **39**, 1397 (1963); P. S. Han, M. F. Rettig, and T. P. Das, Theor. Chim. Acta **16**, 1 (1970).

[26]J. C. Slater and K. H. Johnson, Phys. Rev. B **5**, 844 (1972); K. H. Johnson and F. C. Smith, *ibid.* **5**, 831 (1972).

[27]J. C. Slater, in *Quantum Chemistry,* edited by P. O. Lowdin (Academic, New York, 1972), Vol. 6, p. 1.

[28]For instance, K. J. Duff, Phys. Rev. B **9**, 66 (1974); W. C. Nieuwpoort, D. Post, and P. Th. Van Duijnen, *ibid.* **17**, 91 (1978).

[29]C. Loomis and W. P. Strandberg, Phys. Rev. **81**, 798 (1951).

[30]K. Murakawa, Phys. Rev. **93**, 1232 (1954); **100**, 1363 (1955); G. Sprague and D. H. Tomboulian, *ibid.* **92**, 105 (1953); G. K. Rochester, I. J. Spalding, and K. F. Smith, Philos. Mag. **5**, 1281 (1960).

[31]Mössbauer and nuclear quadrupole resonance data listed by J. G. Stevens and L. H. Bowen, in *Mössbauer Effect Methodology,* edited by I. J. Gruverman (Plenum, New York, 1969), Vol. 5.

[32]C. Svensson, Acta. Crystallogr. Sect. B **31**, 2016 (1975); G. Thronton *ibid.* **33**, 1271 (1977) and references therein.

[33]R. W. Warren *et al.* in Ref. 9.